Supplementary material for:

A satellite-based tool for mapping evaporation in inland water bodies: formulation, application and operational aspects

Matta[a] † E., Amadori[a] †* M., Free[a] G., Giardino[a] C., Bresciani[a] M.

[a] *Institute for Electromagnetic Sensing of the Environment (IREA), National Research Council of Italy (CNR), Via Corti, 12-20133 Milano, Italy*

† These authors equally contributed to this work

**corresponding author*: amadori.m@irea.cnr.it

S1. Heat balance equation

The heat balance equation accounts for all the contributions of thermal energy entering and exiting the water body (Figure 1 in the main text). The energy stored in the water body (Q_x) is the result of a balance between a radiative term (R_n), an advective term (Q_v), and three negative contributions from the fluxes of sensible energy (H), latent energy (λE), and the energy exchanged with the bottom (G). The net radiative term $R_n$represents the residual from the radiative balance at the water/air interface in terms of short (R_s) and long (R_l) wave radiation, considering the incident (i.e. directly coming from the sun, transmitted by the atmosphere, and diffused by the atmosphere), the reflected and the emitted energy from the water body (depending on the water temperature). The advective term Q_v is the net thermodynamic energy flux accounting for the contributions from surface and underground inflows/outflows (F_{in}/F_{out}) and from precipitation (F_p). The sensible energy H is the energy exchanged between the water surface and air due to temperature differences, while the latent energy λE is the energy exchanged during the evaporation process.

In LakeVap we consider the advective energy Q_v and the exchanges with the bottom G to be small compared to the other terms contributing to the net energy stored in the water body. This condition applies to many cases (e.g. [1]. Hence, the energy balance equation in LakeVap is simplified to Equation (S1, i.e. Equation 3 in the main text):

$$Q_x = R_n - H - \lambda E \quad \text{(S1)}$$

where R_n is the radiation at the surface of the water body, H is the sensible energy, and λE is the latent energy.

The R_n term is calculated following Equation (S2)

$$R_n = (1 - \alpha)R_{s\downarrow} + R_{l\downarrow} - (1 - \varepsilon_w) \times R_{l\downarrow} - R_{l\uparrow} \quad \text{(S2)}$$

Where $R_{s\downarrow}$ is the downward shortwave radiation (W/m^2) estimated by meteorological models or measured at meteorological stations, α is the albedo of the water surface, $R_{l\downarrow}$ is the downward longwave radiation, $(1 - \varepsilon_w) \times R_{l\downarrow}$ is the fraction of downward longwave radiation reflected by the water [2] and $R_{l\uparrow}$ is the emitted longwave radiation of the water body. The value of α can be either estimated from the satellite reflectance bands or given as a constant value. In our tool, we verified that there was very little sensitivity to its spatial variations and thus it was fixed at 0.03 based on lake properties (e.g. oligotrophy) and analysis of satellite-derived albedo measures. The downward longwave radiation $R_{l\downarrow}$ (Equation (S3)) and the emitted longwave radiation $R_{l\uparrow}$ (Equation (S4)) are calculated in the LakeVap tool following the Stefan-Boltzmann equation using respectively air and water emissivity ($\varepsilon_a, \varepsilon_w$) and temperature ($T_a, T_w$), with T_w derived from satellite thermal bands (i.e. LSWT).

$$R_{l\downarrow} = \sigma \varepsilon_a T_a^4 \tag{S3}$$

$$R_{l\uparrow} = \sigma \varepsilon_w T_w^4 \tag{S4}$$

In equations (S3) and (S4) $\sigma = 5.67 \cdot 10^{-8}\, W/m^2K^4$ is the Boltzman constant, ε_w= 0.986 is water emissivity [3], and air emissivity ε_a is based on [4] and is dependent on saturated vapor pressure e_{a_sa} and air temperature T_a following Equation (S5) and Equation (S6):

$$\varepsilon_a = 1.24 \left(\frac{e_{a\_sa}}{T_a}\right)^{\frac{1}{7}} \tag{S5}$$

$$e_{a\_sa} = 6.112\, e^{\left(\frac{(17.62T_a)}{(243.12+T_a)}\right)} \tag{S6}$$

The sensible energy is driven by the difference in temperature between the water surface and the air above it (Equation (S7)). In LakeVap we estimate this component as dependent on wind speed u, which can cause air temperature drops and increase the sensible heat exchanges by blowing away the water vapor inside the air.

$$H = \gamma f\, (T_w - T_a) \tag{S7}$$

Where γ = 0.66 is the psychrometric constant and f is an empirical function describing the climatological conditions of the specific study site. In the LakeVap tool the same wind function as that for the latent heat flux is used (see Equation (2) in the main text) by [5] (from [6]):

$$f = 4.8 + 1.98u + 0.28(T_w - T_a) \tag{S8}$$

As already described in the main text, the evaporation heat flux is computed similar to the sensible heat flux by following the formulation of Dalton's law (mass transfer theory) proposed by [5]:

$$\lambda E = f\, (e_w - e_a) \tag{S9}$$

where λ= 2444 kJ/kg is the water latent heat of vaporization. Hence, in our tool, evaporation is proportional to the vapor pressure gradient between air at the air-water interface and air at 2 m a.w.l. $(e_w - e_a)$, to wind speed

and to the thermal difference between water and air. The vapor pressure at air temperature (e_a) is calculated multiplying the saturated vapor pressure $\left(e_{a\_sa}\right)$ at air temperature T_a by the relative humidity of air (RH), Equation (S10)). Vapor pressure at the air-water interface (e_w) is assumed saturated and at the same temperature as water and is calculated following [5] as in Equation (S11)):

$$e_a = e_{a\_sa}\frac{RH}{100} \tag{S10}$$

$$e_w = 6.112\, e^{\left(\frac{(17.62T_w)}{(243.12+T_w)}\right)} \tag{S11}$$

Table S1 shows a summary of all the variables used in the LakeVap tool.

Table S1: List of variables used in the LakeVap tool, equation numbers where variables appear and variable type (input (I), output (O), variables derived from a combination of other variables (D), and constant values (C)).

Symbol	Definition	Equation	I/O/D/C
Q_x	Energy stored in the water body (W/m^2)	(3), (4), (S1)	D
R_n	Net radiation at the surface of the water body (W/m^2)	(3), (S1), (S2)	D
H	Sensible heat (W/m^2)	(3), (S1), (S7)	D
λE	Latent heat (W/m^2)	(3), (S1), (S9)	O
λ	Water latent heat of vaporization (kJ/kg)	(3), (S1), (S9)	C
α	Albedo of the water surface	(S2)	C
$R_{s\downarrow}$	Downward shortwave radiation (W/m^2)	(S2)	I
$R_{l\downarrow}$	Downward longwave radiation (W/m^2)	(S2), (S3)	D
$R_{l\uparrow}$	Emitted longwave radiation (W/m^2)	(S2), (S4)	D
σ	Boltzmann constant (W/m^2K^4)	(S3), (S4)	C
ε_a	Air emissivity	(S3), (S5)	D
ε_w	Water emissivity	(S2), (S4)	C
T_a	Air temperature (°C or K)	(S3), (S5), (S6), (S7), (S8)	I
T_w	Water temperature (°C or K)	(S4), , (S7), (S8), (S11), (4), (5)	I
e_{a_sa}	Saturated vapor pressure (mb)	(S5), (S6), (S10)	D
γ	Psychrometric constant	(S7)	C
f	Wind function	(1), (2), (S7), (S8)	D
e_w	Vapor pressure at air/water interface (mb)	(S9), (S11)	D
e_a	Vapor pressure at air temperature (mb)	(S9), (S10)	D
u	Wind speed (m/s)	(2), (S8)	I
RH	Relative humidity (%)	(S10)	I
ρ_w	Density of water (kg/m^3)	(S12)	C
c_p	Specific heat of water ($kg^{-1}\ K^{-1}$)	(S12)	C
z	Thickness of the surface water level (m)	(S12)	C
E_h	Instantaneous evaporation rate (mm/h)	(6), (S12)	O
E_d	Daily evaporation rate (mm/day)	(6)	O

S2. Sensitivity of evaporation estimates to meteorological variables

S2.1 Setup of sensitivity tests

In order to understand what atmospheric variable plays the major role in influencing the estimates of instantaneous evaporation, a sensitivity analysis of the LakeVap tool was performed. The ensemble used for this analysis is reported in the main text on Section 2.4. For easing the comprehension of the results reported in this SI, we summarize here the key points.

LakeVap was forced by a wide range of atmospheric forcing based on the time series of WRF spatially resolved fields of air temperature, relative humidity and wind. The LakeVap ensemble comprises four sets (items 5 and 6 in Section 2.4). Each set is composed by the LakeVap estimations of evaporation for all dates when CCI-Lakes LSWT maps meet the quality requirements detailed in Section 2.3.1. The first set (item 5 in the list in Section 2.4) is the reference set obtained by imposing all WRF meteorological data as spatially averaged over the lake surface. In the remaining three sets (item 6 in Section 2.4) we apply one of the three atmospheric variables at time as spatially varying (e.g. air temperature), while the other two (e.g. wind speed and relative humidity) are kept as uniform over the lake.

In this way, each instantaneous evaporation map from the given set represents a sample of I pixels (i.e. the total number of pixels within a single map) sensitive to a variation of the given meteorological variable. For each date (n), a rate of variation is computed on each pixel (i) for both the estimated instantaneous evaporation (E_h) and meteorological variable (M) imposed as spatially varying, following an approach similar to that of equation 16 in the main paper:

$$\Delta {E_h}^{n,i} = \frac{E_h^{n,i} - E_h^{n,R}}{E_h^{n,R}} \cdot 100 \quad \text{(S12)}$$

$$\Delta M^{n,i} = \frac{M^{n,i} - M^{n,R}}{M^{n,R}} \cdot 100 \quad \text{(S13)}$$

Where the reference for the two variations are the estimates of evaporation obtained with spatially averaged meteorological forcing for the n -day ($E_h^{n,R}$) and the averaged meteorological forcing itself ($M^{n,R}$).

The sensitivity analysis is thus performed by correlating $\Delta {E_h}^{n,i}$ and $\Delta M^{n,i}$.

The investigated range of variation resulting from our sample of WRF fields covers a window of 150%. This means that we evaluated the effect of adopting a meteorological variable up to 3 times larger/smaller than the reference one, as this is indeed the order of magnitude of the maximum difference among the examined meteorological datasets (see Section 3.2 in the

main paper). It is worth noting that such range is way narrower than the range of variation of both evaporation and meteorological variables (wind and air temperature especially) on a seasonal basis. In fact, the reference value used to compute the percentage variation in Equation (S12) and Equation (S13) (i.e. $E_h^{n,R}, M^{n,R}$) has a seasonal behavior, which is removed by the subtraction to the time-dependent $E_h^{n,i}$ and $M^{n,i}$, respectively.

S2.2 Results

In Figure S1 the results of such sensitivity analysis are presented. In panel a) we report the percentage variation of evaporation estimate due to the variation of each meteorological forcing. Such variation is presented in terms of the mean value over all pixels and dates of $\Delta {E_h}^{n,i}$ from Equation (S12) (colored bars) and its standard deviation (error bars). In panel b) we report the statistical distribution of $\Delta M^{n,i}$.

a)

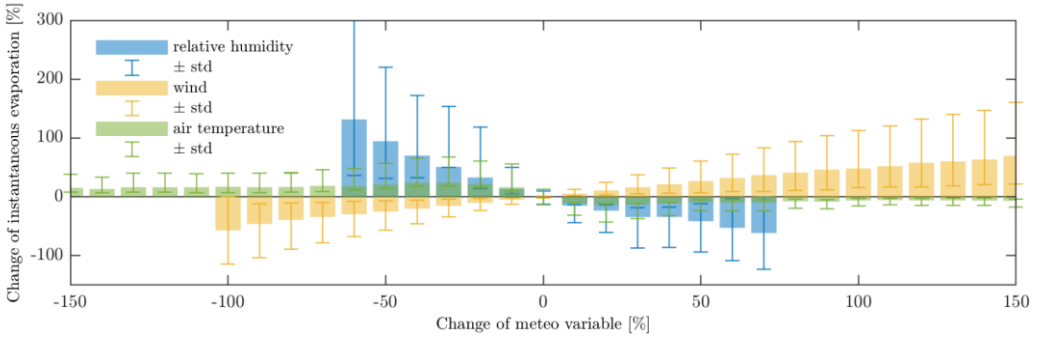

b)

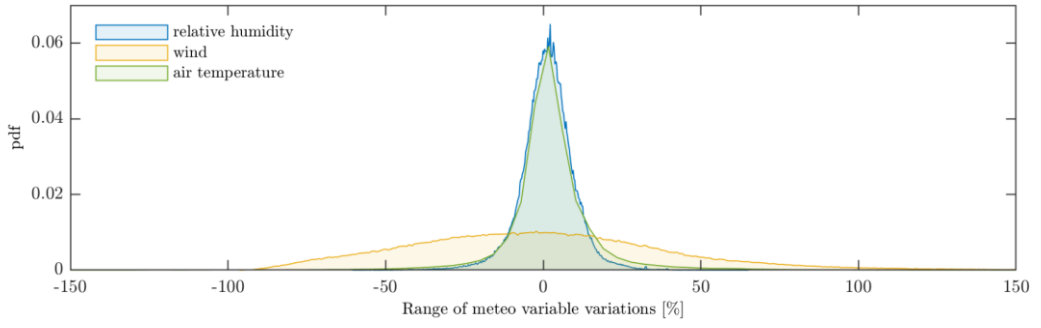

Figure S1 a) Percentage of variation of evaporation estimates due to the variation of each meteorological variable computed as the mean deviation from the reference value on each time step and on each pixel of the map, normalized by the reference value (equations (S12) and (S13)). The error bars indicate the standard deviation of the evaporation change. b) Investigated ranges of meteorological variables in terms of probability distribution of percentage variation with respect to the reference value.

The evaporation estimated with LakeVap shows a limited sensitivity to the air temperature, with over/underestimations of the instantaneous evaporation rate of the order of 16-20% even when air temperature is two (100%) or three (150%) times larger/smaller than the reference value. On the contrary, relative humidity has a significant impact on the value of instantaneous evaporation: over/underestimations of the 60% lead to over/underestimations of the instantaneous evaporation over ±100%. As expected, evaporation is anticorrelated with these two variables if LSWT remains unchanged: indeed, evaporation increases if air temperature and relative humidity decrease. However, air temperature and relative humidity variations typically range within an interval of ±20% in the lake (Figure S1b), and among the datasets (Figure 6). Within this interval, the rate of change of evaporation is approximately of the same order of magnitude, hence the spatial variability of these two atmospheric variables has limited impact on the estimated instantaneous evaporation. The sensitivity to wind speed linearly grows with its variation. Despite such sensitivity looks comparable or smaller than that to relative humidity within a range of ±60%, it has more effects on the estimation of instantaneous evaporation as the range of variation of wind speed is wider (Figure S1b). We have indeed seen in Figure 6 that wind speed is significantly underestimated by ERA5 and only partially represented by either WRF, MET1 and MET2, as it is strongly dependent on the local climatic conditions. Hence, a misrepresentation of this weather forcing in the test site leads to underestimating the instantaneous evaporation rate of up to 3 times.

References

1. Gianniou, S.K.; Antonopoulos, V.Z. Evaporation and Energy Budget in Lake Vegoritis, Greece. *J. Hydrol.* **2007**, *345*, 212–223, doi:10.1016/j.jhydrol.2007.08.007.
2. Allen, R.G.; Tasumi, M.; Trezza, R. Satellite-Based Energy Balance for Mapping Evapotranspiration with Internalized Calibration (METRIC)—Model. *J. Irrig. Drain. Eng.* **2007**, *133*, 380–394, doi:10.1061/(ASCE)0733-9437(2007)133:4(380).
3. Wukelic, G.E.; Gibbons, D.E.; Martucci, L.M.; Foote, H.P. Radiometric Calibration of Landsat Thematic Mapper Thermal Band. *Remote Sens. Environ.* **1989**, *28*, 339–347, doi:10.1016/0034-4257(89)90125-9.
4. Brutsaert, W. On a Derivable Formula for Long-Wave Radiation from Clear Skies. *Water Resour. Res.* **1975**, *11*, 742–744, doi:10.1029/WR011i005p00742.
5. Fink, G.; Schmid, M.; Wahl, B.; Wolf, T.; Wüest, A. Heat Flux Modifications Related to Climate-Induced Warming of Large European Lakes. *Water Resour. Res.* **2014**, *50*, 2072–2085, doi:10.1002/2013WR014448.
6. Livingstone, D.M.; Imboden, D.M. *Annual Heat Balance and Equilibrium Temperature of Lake Aegeri, Switzerland*; 1989; Vol. 51;.